NJC

Accepted Manuscript

This is an *Accepted Manuscript*, which has been through the Royal Society of Chemistry peer review process and has been accepted for publication.

Accepted Manuscripts are published online shortly after acceptance, before technical editing, formatting and proof reading. Using this free service, authors can make their results available to the community, in citable form, before we publish the edited article. We will replace this *Accepted Manuscript* with the edited and formatted *Advance Article* as soon as it is available.

You can find more information about *Accepted Manuscripts* in the Information for Authors.

Please note that technical editing may introduce minor changes to the text and/or graphics, which may alter content. The journal's standard Terms & Conditions and the Ethical guidelines still apply. In no event shall the Royal Society of Chemistry be held responsible for any errors or omissions in this *Accepted Manuscript* or any consequences arising from the use of any information it contains.

ROYAL SOCIETY OF CHEMISTRY

www.rsc.org/njc

NJC

RSCPublishing

PAPER (or FOCUS or PERSPECTIVE)

An activated coumarin-enamine Michael acceptor for CN^-

Cite this: DOI: 10.1039/x0xx00000x

Aaron B. Davis[(a)], Rachel E. Lambert[(a)], Frank R. Fronczek[(b)], Peter J. Cragg[(c)] and Karl J. Wallace*[(a)]

Received 00th January 2012,
Accepted 00th January 2012

DOI: 10.1039/x0xx00000x

www.rsc.org/

Abstract: Two coumarin-enamine chemodosimeters have been synthesized in three steps. They have been shown to selectively detect the cyanide ion with a fluorescent response ($t_{½}$ = 20 s) and a limit of detection approximately 4.2 ppb in DMSO. The X-ray crystal structure of the thermodynamically stable *E*-(keto) enamine isomer of one compound was obtained and exhibited offset π-stacking.

Introduction

Anion recognition is now a well-established area of research, so much so that Gale has written regular updates on the area over 10 years.[1-6] One aspect of anion recognition of practical importance is the design and synthesis of molecular probes to detect and monitor anions by colorimetric[7], fluorescent[8] or electrochemical[9] means, however, the main challenges to the design of molecular probes are sensitivity and selectivity. One of the most interesting but "simple" anions to monitor is the cyanide ion due to its environmental[10], biological[11] and industrial importance.[12] The specific challenge of cyanide detection is a consequence of the different species that exist in solution. At a pH of 9.3 - 9.5, CN^- and HCN are in equilibrium, with equal amounts of each present, referred to as free cyanide. At a pH of 11, over 99% of the cyanide remains in solution as CN^- known as the cyanide ion, while at pH 7, over 99% of the cyanide will exist as molecular cyanide, HCN. Other species that exist that are prevalent in the mining industry are simple cyanides (i.e., KCN), complex cyanides (i.e., $Ag(CN)_2$), weak acid dissociable cyanides, e.g., $Cd(CN)_2$) and strong acid dissociable cyanides, e.g., ($Co(CN)_6^{4-}$). The summation of these cyanide species is known as the total cyanide concentration.[13]

The cyanide ion displays an intrinsic nucleophilic behavior towards carbon centers, particularly carbonyl groups, e.g., aldehydes[14], iminium groups [15] and carbon-carbon double bonds[16-18], as well as Lewis acid centers.[19] Needless to say these functional groups have been incorporated into colorimetric, fluorescent and electrochemical molecular probes that detect cyanide. A recent review by Yoon *et al* highlights some elegant examples of such sensors.[20]

Derivatives of 1,2-benzopyrone (commonly known as coumarin) have been used extensively as molecular probes due to their unusual photophysical properties in different media.[21] As a consequence, numerous coumarin molecular probes have been utilized as colorimetric and fluorescent sensors.[8, 15, 17, 21-23] Although a recent coumarin-enamine derivative was used in the histochemical identification of β-amloid plaque[24], the use of coumarin enamine molecular probes is not particularly prevalent in the realms of anion recognition.

As part of our ongoing interest in the design of new molecular probes, we have synthesized coumarin enamines **3** and **4** (Figure 1) that can undergo Michael addition of cyanide at the α, β-unsaturated carbonyl. It is well known that electron withdrawing functional groups attached to a carbonyl moiety will pull electron density away from the carbon atom. Consequently making this region more electrophilic will render it more susceptible towards rapid nucleophilic attack. Our intention was also to synthesize a planar molecular with a high degree of conjugation which can be easily perturbed to produce a spectroscopic response. Thus we took advantage of intramolecular hydrogen bonding, available to **3** and **4**, that forms a resonance assisted hydrogen bonding interaction (RAHB).[25] Upon addition of the cyanide it was anticipated that a significant spectroscopic response in the UV-vis and fluorescence

spectra would occur through perturbation of chemodosimeter conjugation. To the best of our knowledge this is the first time that a coumarin-enamine scaffold has been used to detect cyanide ions in this manner.

Results and Discussion

Synthesis and Crystallography Studies

The two coumarin-enamine compounds were prepared in three straightforward steps (Scheme S1, ESI). Solution studies on **3** showed that the product existed as a mixture of two *E* and *Z* isomers in a solvent independent 1:3 ratio. Tautomeric transformations can also occur, (Scheme S2, ESI), however the *E*-(keto) enamine and *Z*-(keto) emamine, were the only species observed in solution.

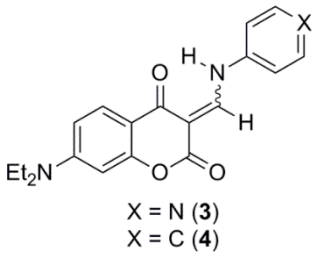

Fig 1. Coumarin-enamine target chemodosimeters.

Fortunately, X-ray quality crystals of *E*-**3** were obtained by heating a concentrated solution of **3** in DMSO and allowing it to stand for several days. Even though DMSO is known as a competitive solvent, and often hinders hydrogen bonding interactions, the crystal packing of **3** is dominated by two sets of bifurcated hydrogen C-H···O interactions between C(10)-H and C(12)-H of *E*-(keto)-enamine **3** and the O(2) of an inversion-related molecule that is in the *anti*-orientation (Figure 2). The crystal packing shows that each molecule is offset such that the electron rich aniline B ring system (Scheme 1) is stacked *via* a π-π arrangement with the electron deficient enamine-derived A ring system with a separation of 3.64 Å (Fig, S1(b), ESI), which is in excellent agreement with other aromatic stacking arrangements.[26] The planarity of the molecular probe is also stabilized by a very strong intramolecular hydrogen bonding interaction between N(1)-H···O(3) at 1.95(3) Å, in essence forming a pseudo ring system.

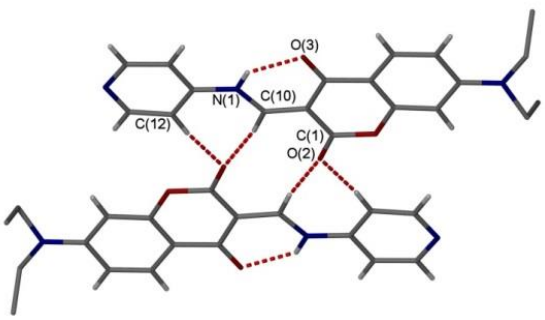

Fig 2. Crystal structure of **3**, illustrating the two set of bifurcated hydrogen bonding interactions (dashed lines). Donor-acceptor distances (Å): intramolecular hydrogen bond N(1)-H(1)N···O(3) = 2.642(2); intermolecular hydrogen bond C(10)-H(10)···O(2) = 3.342(3) and C(12)-H(12)···O(2) = 3.191(3).

UV-Vis and Fluorescence Spectroscopic Studies

There have been many studies on the photophysics of coumarin molecules and it is well known that changes in the dipole moment of these molecules significantly influences the Stokes shift depending on the polarity of the solvent. This has led to some very unusual photophysical behavior.[21, 22] The spectroscopic responses of many molecular probes are often only investigate in one particular solvent system, normally a water-organic solvent mixture, presumably to show that a particular system works in water-based environments; more often than not other solvent systems are ignored. Therefore, before we investigated the response between **3** and **4** towards various anions, we examined the basic photophysical properties in a range of nonpolar to polar solvents. A plot of solvent polarity factor, ΔF, against absorption and fluorescence λ_{max} values for **3** is shown in the ESI Fig. S3(A). The hypsochromic shift observed in the UV-vis spectra as solvent polarity increases (negative solvatochromism) is a consequence of the ground state of **3** being stabilized by the solvent than the excited state. There was no effect on **4** as the ring system contains a carbon atom instead of the nitrogen atom. However, the λ_{fl} (Fig. S3(B), ESI red line) exhibits a greater solvent effect and a bathochromic shift as the polarity increases, this is seen for both **3** and **4** (Fig. S3, ESI). This is in excellent agreement with coumarin dyes with a dialkylamino group tethered at the 7-position on the coumarin scaffold and has been attributed to the stabilization of the intramolecular charge transfer (ICT), in turn leading to stabilization of the excited singlet state.[22] The more non polar the solvent the more a blue/green the fluorescence emission appears under a UV lamp (Fig. S2, ESI).

After investigating the photophysical properties in the different solvent systems, we decided to use one with an uncomplicated spectroscopic signal. The spectroscopic behavior of **3** and **4** towards a number of monoanionic analytes was determined in DMSO. Potassium cyanide was chosen to ensure complete dissociation in the solvent. Upon the addition of CN^- a distinct change can be observed from a yellow to colorless solution (Figure 3 B), whereas the color intensity for the other anions remained unchanged, with the exception of the fluoride (Figure 3 C) and acetate ions (Figure 3 N). These two exceptions may result from the two anions' hydrogen bonding and inhibition of the excited state intramolecular proton transfer (ESIPT) mechanism as proposed in the literature.[27-29] However, a more likely explanation is that partial deprotonation is responsible for the spectroscopic change as both the fluoride anion and acetate anion are basic in DMSO solution and the abstraction of a proton by both of these anions is a well-known phenomenon in supramolecular chemistry.[30]

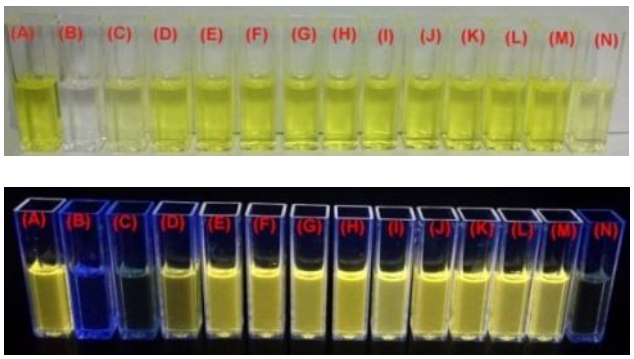

Fig 3. (Top) Colorimetric response via naked eye in DMSO (Bottom) under the UV-lamp: Probe **3** (0.2 moldm^{-3}) and anions (0.3 moldm^{-3}); (A) compound **3** (B) KCN (C) TBAF (D) $TBAH_2PO_4$ (E) TBABr (F) TBACl (G) TBAI (H) $TBANO_3$ (I) $NaBF_4$ (J) NaN_3 (K) $TBAHSO_4$ (L) NH_4SCN (M) $NH_4ClO_4^-$ (N) $TBACH_3CO_2$.

The UV-vis absorption spectra of all the anions studied is shown in the Supporting Information (Fig. S4, ESI). Compound **3** shows a broad band at 405 nm that is shifted on the addition of CN^-, with the appearance of a hyperchromic band at 335 nm through a well-defined isosbestic point at 340 nm (Figure 4 top insert). The absorption band at the longer wavelength can be attributed to resonance assisted hydrogen bonding, which in essence means that there are four ring systems that span the molecule. On the addition of the nucleophile to the enamine ring C is broken, thus the conjugation is hampered due to the hybridization change from sp^2 to sp^3 (Scheme 1).

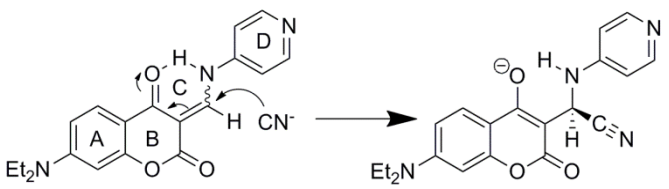

Scheme 1: The proposed Michael addition of the CN^- breaking up the pseudo conjugated molecular probe **3** and perturbing the delocalisation due to the hybridization change.

The UV-vis spectrum of the fluoride does show some similar spectroscopic changes, whereas octylamine spectrum shows a very different response (Fig S4, ESI) with a new band appearing at 365 nm. It is reasonable to believe that this new species is a consequence of an acid base reaction whereby the primary amine has deprotonated the molecule in the *E-s-cis*-hydroxyimine form, thus significantly changing the electronics of the system. A plot of the absorbance ratio at 335/405 nm upon the addition of two equivalents of KCN shows that the ratiometric response towards CN^- is approximately six times greater than the fluoride ion (Figure 4, top). Even though there was a response on the addition of cyanide we wanted to see if the two anions can be further distinguished and turned to the more sensitive technique of fluorescence spectroscopy (Fig. S6 and S8, ESI for all anions). Upon the addition of cyanide the florescence spectrum exhibited an emission shift of 219 nm with an isoemissive point at 475 nm. A plot of the nominalized fluorescence ratio at 356/575 nm upon the addition of two equivalents of KCN shows a clear response towards cyanide, over the other anions studied, by a factor of 350 (Figure 4, bottom).

As we could clearly distinguish CN^- in the fluorescence spectrum we used fluorescence spectroscopy to determine the limit of detection (LOD) of cyanide upon reaction with **3,** a key requirement for any molecular probe for cyanide. The LOD was determined by least squares linear regression. The confidence limit of the slope is defined as $b \pm t_{sb}$, where t is the t-value taken from the desired confidence level and n-2 degrees of freedom; here a 98% confidence level (t-value 2.72, df = 11) was adopted (Fig. S33, ESI). It is generally accepted that the LOD is the analyte concentration giving a signal equal to that of the blank signal plus three standard deviations from the blank, i.e. $y = y_B + 3S_B$. The LOD values for chemodosimeter **3** were calculated to be 4.2 ppb, in the range of other examples[31, 32] and well below the threshold set by the European Union (50 ppb) and the United States (200 ppb). Interestingly, the guidelines set by WHO in 2011 stated that it is not necessary to establish short-term detection limits of cyanide ions in drinking water due to the rapid detoxification by the liver.[33] However, the guidelines do point out that high doses can give rise to thyroid toxicity.[33, 34] which is of particular importance in developing countries due to the lucrative business of gold mining that requires cyanide as part of the gold extraction process. To confirm that the cyanide ion added to the chemodosimeter in a 1:1 manner, we ran Job plot analysis and ESI-MS (SI Figures S32 and S8 respectively); the Job plot showed that the mole fraction was at 0.5 and a m/z = 363 assigned to the $[M\text{-}CN]^-$ signal. We then undertook an extensive NMR investigation on **3**.

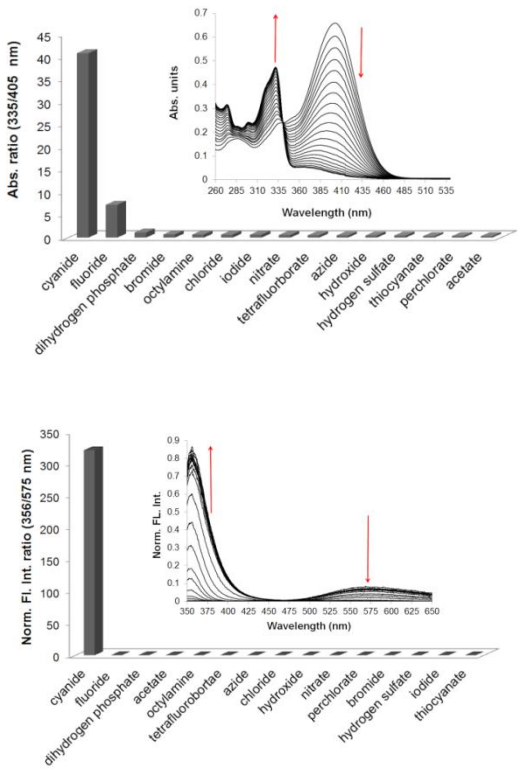

Fig 4. UV-Vis titration of **3** (16 mmoldm^{-3}; DMSO, λ_{Ex} 339 nm) upon the addition of two equivalents of KCN (top). The bar plot illustrates the ratiometric response of probe **3** in the presence

of the anions studied (two equivalents); Normalized fluorescence titration data of probe **3** (0.16 moldm^{-3}), upon the addition of two equivalent KCN (bottom).

NMR Studies

The enamine can exist as two geometrical isomers (*E* or *Z*) or one of a plausible number of tautomers (Fig. S35, ESI). No tautomers were detected in the NMR spectra; only the *E*-(keto) enamine and the *Z*-(keto) enamine isomers of **3** were evident. Integration of the ^{1}H NMR showed a 3:1 ratio for *E*-(keto) enamine and the *Z*-(keto) enamine respectively, in a mixture of $CHCl_3$-*d*:DMSO-d_6 (6:1), consistent with other coumarin enamines.[35] The *E* isomer was found to be lower in energy than the *Z* and the only product that formed X-ray quality crystals. As the UV-Vis and fluorescence data showed an optical response upon the addition of KCN, we investigated the change in the NMR spectra upon the addition of 1.2 equivalents of KCN to **3**.

Due to the poor solubility of KCN in $CHCl_3$ 100% DMSO-d_6 was used for the NMR studies. As a consequence of the 1,4 addition of cyanide the *E* and *Z* isomers no longer exist in solution so both ^{1}H and ^{13}C spectra became significantly easier to assign (Figure 5). Interestingly, there is only one addition product observed in the NMR. The two downfield doublets at δ 11.52 and 13.50 ppm *Z*-**3** and *E*-**3** respectively are assigned to the NH proton, confirmed by HSCQ (Fig. S19, ESI). As these signals were not correlated to any corresponding carbon atoms, and they also disappeared upon a D_2O shake. Both of these signals subsequently disappeared upon the addition of cyanide with a new sharp doublet appearing at δ 6.95 ppm. The ^{13}C NMR was significantly more informative, in particular the ^{13}C APT spectrum which distinguishes between CH/CH_3 (positive signals) and CH_2/C (negative signals). Upon the addition of the cyanide C(3) and C(9) are observed at δ 99.2 (*E*-**3**); 99.7 (*Z*-**3**) and 151.8 ppm which shifted up-field to δ 88.0 and 125.0 ppm C(3) and C(9) respectively and the quaternary carbon atom of the cyanide is seen as a negative signal at 119.5 ppm in the ^{13}C ATP experiment (Fig. S27, ESI).

Computational Studies and Kinetic Anlaysis

Computational methods were used to calculate eight different conformers of **3** in the gas phase (Fig. S35, ESI structures A to H). From the NMR of **3** and the product formed from the reaction with cyanide the only structures that could be involved were that shown in Figure 1, with the N-H *Z* to the ketone, and its *E* isomer. Of these, the former was preferred on energetic grounds.

A sequence of structures was generated in which CN^- approached the target carbon down a vector. A reaction trajectory was attempted using DFT/B3LYP/6-311G* but simulations resulted in proton abstraction rather than cyanide addition so a simpler method was employed. A PM6 semi-empirical simulation was more successful, indicating that there were no orbital interactions between CN^- and the target at distances exceeding 3.14 Å. This was taken as a starting point and the C-CN distance was reduced in steps of 0.33 Å down to 1.48 Å which had been identified as the optimum C-CN bond distance from a DFT/B3LYP/6-311G* calculation. The effect that this has on the HOMO of the system is illustrated in Figure 6. As expected, electron density is initially associated with the incoming cyanide but, as a C-C bond is formed, this migrates to the coumarin region of probe **3**.

The cyanide ion is known to stop cellular respiration by inhibiting the cyctochrom C oxidase enzyme at high concentrations.[36] Therefore it is imperative that the detection of the cyanide ion is achieved quickly. As pyridine groups are more electron withdrawing than the analogous benzene group we anticipated that the kinetics between compound **3** would occur faster than probe **4**, as the electron density is being pulled away from the enamine carbon making it more electrophilic for the nucleophile to attack. Our initial studies indicate that this is true. A 2.5×10^{-5} mol dm^{-3} solution of **3** and a 1.25×10^{-4} mol dm^{-3} solution of KCN were mixed in equal amounts and the reaction was monitored for 3 min. at 335 nm. Pseudo first-order kinetics were assumed and, by monitoring the increase at 335 nm over time, the rate of the reaction was calculated from $\ln(A_o/(A_o - A_I))$ versus time (SI Figure S34), where A_o is the final absorbance intensity and A_I is the absorbance intensity recorded at each time interval measured. The rate constant, *k*, was calculated to be 0.03 s^{-1} giving a half-life ($t_{½} = \ln 2/k$) of approximately 23 seconds. We are currently investigating the kinetics of a number of different substituted isomers containing electron withdrawing and donating groups to increase the rate of reaction.

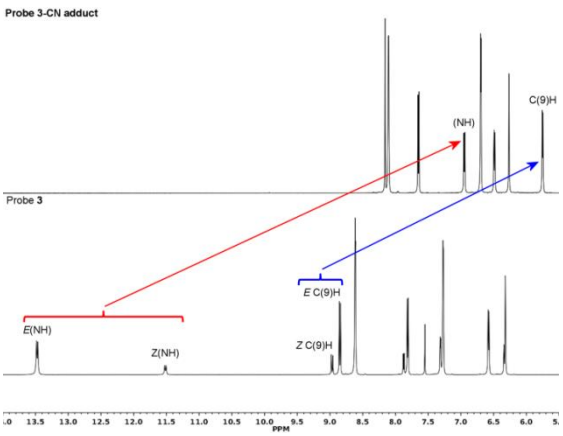

Fig 5. ^{1}H NMR spectral change of the dosimeter **3** (DMSO, 9.5 mM) on the addition of 1.2 equivalents of KCN (DMSO, 7.6 mM).

Conclusions

In summary, two coumarin-enamine dyes have been synthesized and their spectroscopic behavior, in particular fluorescence, has demonstrated their selectivity for CN^- over 12 common anions with a LOD in the region of 4 ppb. Michael reactions are reversible under certain conditions, yet we were unable to observe any reversibility in our probes, despite numerous attempts achieve this. Therefore, the current probes act as true, stable chemodosimeters. We have also investigated the spectroscopic properties in various organic solvents, something that is often omitted in the published literature. Despite a spectroscopic response from F^- and $CH_3CO_2^-$, which is most

likely due to partial deprotonation, we now have a good understanding that these molecules can be used to detect cyanide ions, we are currently incorporating ting them into "test strips" and incorporating them into polymeric matrices for onsite detection of hydrogen cyanide in air.

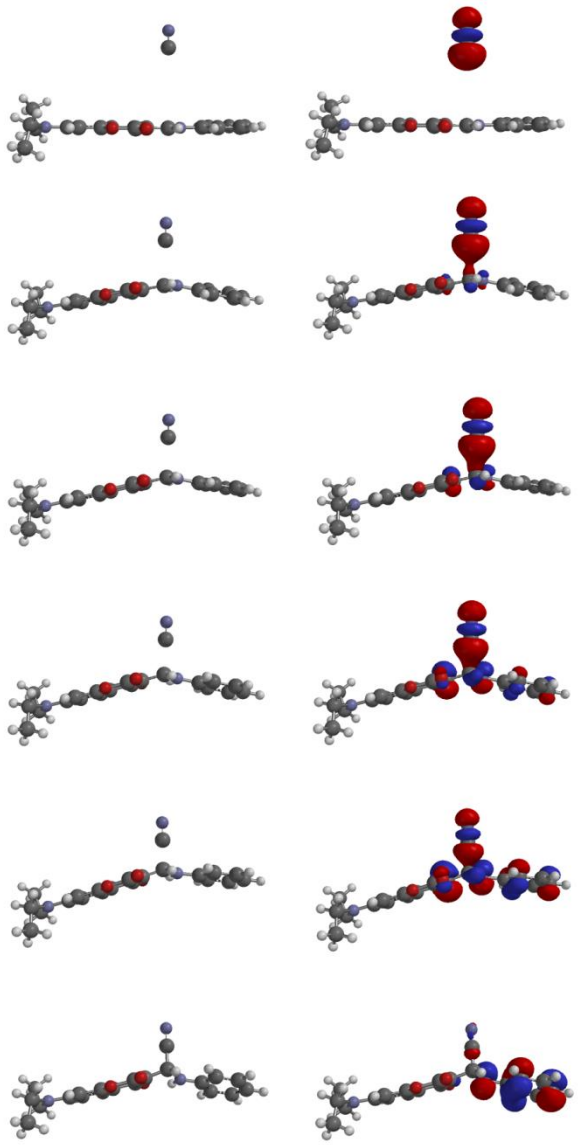

Fig 6. Reaction between cyanide and **3** as calculated by DFT (B3LYP/6-311G*): NC···C distance (from top) 5.00Å, 3.15 Å, 2.80 Å, 2.48 Å, 2.15 Å, 1.80 Å and 1.48 Å. Structures (left) are shown superimposed with HOMOs on the right (see Supplementary Information for details).

Experimental

General techniques: One-dimensional (^{1}H, ^{13}C and ^{13}C APT) and two-dimensional (HMBC, HSQC and ROESY) NMR spectra were recorded Bruker Avance 600 spectrometer operating at a proton frequency of 600.13 MHz and equipped with a standard BFO 5 mm two channel probe in the appropriate deuterated solvents or were recorded on a Bruker Ultrashield plus 400 MHz spectrometer. Chemical shifts are reported in parts per million (ppm) downfield from tetramethylsilane (0 ppm) as the internal standard and coupling constants (*J*) are recorded in hertz (Hz). The multiplicities in the ^{1}H NMR spectra are reported as (br) broad, (s) singlet, (d) doublet, (*dd*) doublet of doublets, (*ddd*) doublet of doublet of doublets, (*t*) triplet, (*sp*) septet and (*m*) multiplet. All spectra are recorded at ambient temperature, unless otherwise stated. UV-Vis experiments were performed on a Beckman DU-70 UV-Vis spectrometer. Low resolution mass spectra were measured with Finnigan TSQ70 IR spectra were recorded on a Nicolet Nexus 470 FT-IR paired with a Smart Orbit ATR attachment. The characteristic functional groups are reported in wavenumbers (cm^{-1}), and are described as weak (w), medium (m), strong (s) and very strong (vs). Fluorescence experiments were carried out on a QuantaMasterTM 40 intensity based spectrofluorometer from PTI technologies in the steady-state. High resolution mass spectra (HRMS) were recorded at the Department of Chemistry at University of Alabama, Tuscaloosa. X-Ray crystallography was carried in in the department of chemistry at Louisiana State University, see page 42-46 in ESI for experimental details, crystal data and tables.

Synthesis and characterization:

Synthesis of *bis*-(2,4,6-trichlorophenyl)malonate (1)[23, 24]: 2,4,6-Tricholorphenol (15.8 g, 79.8 mmol), malonic acid (4.16 g, 39.9 mmol) and phosphorus (V) oxychloride (10 mL, 107 mmol) were refluxed for three hours. The reaction was allowed to cool to room temperature and quenched with cold deionized water (50 mL). The precipitate was collected and dissolved in deionized water (10 mL). The solution was then brought to pH = 7 by the addition of saturated sodium bicarbonate solution. The resulting solid was collected by vacuum filtration and recrystalized from ethylacetate (16.6 g, 90 % yield). ^{1}H NMR (300 K, DMSO-d_6, 400 MHz): δ 7.53 (*s*, 4H, ArH), 3.85 (*s*, 2H, CH_2); ^{13}C NMR (300 K, DMSO-d_6, 100 MHz): 168.8, 149.0, 128.6, 123.8, 123.5.

Synthesis of 7-(diethylamino)-4-hydroxycoumarin (2)[23]:

Bis-(2,4,6-trichlorophenyl)malonate (9.26 g, 20.0 mmol) and 3-diethylaminophenol (3.30 g, 20.0 mmol), and anhydrous toluene (50 mL) were refluxed for three hours. The reaction was allowed to cool to room temperature. The precipitate was collected by vacuum filtration and washed with toluene (3.50 g, 75 % yield). ^{1}H NMR (300 K, DMSO-d_6, 400 MHz): 11.91 (*s*, 1H, OH), 7.55 (*d*, 1H, *J* = 9.0 Hz, ArH), 6.65 (dd, 1H, *J* = 9.0 and 2.2 Hz, ArH), 6.45 (d, 1H, *J* = 2.2 Hz, ArH), 5.25 (s, 1H, CH), 3.42 (d*q*, 4H, *J* = 14.0 and 7.0 Hz, CH_2), 1.11 ppm (*t*, 6H, *J* = 7.0, CH_3); ^{13}C NMR (300 K, DMSO-d_6, 100 MHz): 166.9, 163.2, 156.6, 151.3, 124.6, 108.6, 103.9, 98.9, 86.6, 44.4, 12.8.

General procedure for molecular probes (3) and (4): 7-(Diethylamino)-4-hydroxycoumarin (**2**) (1.0 mmol), and the appropriate primary amine (1.0 mmol), and triethylorthoformate (1.5 mmol) were refluxed in propan-2-ol (5 mL) for two hours. The reaction was allowed to cool to room temperature. The resulting solid was collected by vacuum filtration and washed with cold propan-2-ol (typical yields 80 to 85%).

Characterization of probe (3): Yield 282 mg, 0.84 mmol, 84 % yield; ^{1}H NMR (300 K, DMSO-d_6, 600 MHz) and ^{13}C NMR (300 K, DMSO-d_6, 150 MHz): See pages 15-27 for 1D and 2D spectrum. ESI-MS; m/z for $[M+H]^+$ = 338.2; IR (ATR solid);

3059 (w) $\nu_{C=C(enamine)}$, 2970 (w) ν_{CH}, 1716 (s) νCO (delta lactone), 1571 νCO (ketone) cm^{-1}; HRMS observed for $C_{19}H_{19}N_3O_3$ = 337.1430; Calculated for $C_{19}H_{19}N_3O_3$ = 337.1426

Characterization of probe (4): Yield 268 mg, 0.98 mmol, 80 % yield; ^{1}H NMR (300 K, $CHCl_3$-*d*, 400 MHz): δ 13.65 (*d*, 1H, *J* = 12.5 Hz, NH), 8.82 (*d*, 1H, *J* = 13.3 Hz, $CH_{enamine}$), 7.87 (*d*, 1H, *J* = 9.0 Hz, $CH_{coumarin}$), 7.45 (*t*, 2H, *J* = 7.9 Hz, $CH_{aromatic}$), 7.30 (*dt*, 3H, *J* = 15.9 and 7.5 Hz, $CH_{aromatic}$), 6.59 (*dd*, 1H, *J* = 9.0 and 2.4 Hz, $CH_{coumarin}$), 6.38 (*d*, 1H, *J* = 2.3 Hz, $CH_{coumarin}$), 3.45 (*q*, 4H, *J* = 7.1 Hz, CH_2), 1.15 ppm (*t*, 6H, *J* = 7.1 Hz, CH_3); ^{13}C NMR (300 K, $CHCl_3$, 100 MHz): 181.0, 164.5, 157.2, 153.5, 152.9, 138.2, 130.8, 127.3, 126.6, 118.0, 108.8, 108.4, 98.1, 97.2, 44.9, 12.9; ESI-MS m/z $[M+H]^+$ = 337.0; IR (ATR solid) IR (ATR solid); 3239 (w) ν_{NH} 3059 (w) $\nu_{C=C(enamine)}$, 2970 (w) ν_{CH}, 1716 (s) νCO (delta lactone), 1571 νCO (ketone) cm^{-1}; HRMS observed for $C_{20}H_{20}N_2O_3$ = 336.1484; Calculated for $C_{19}H_{19}N_3O_3$ = 336.1474

Acknowledgements

The KJW group is grateful for the financial support from NSF Grant OCE-0963064.

Notes and references

[a] Department of Chemistry and Biochemistry University of Southern Mississippi, Hattiesburg, Mississippi 39406, United States.

[b] Department of Chemistry, Louisiana State University, Baton Rouge, Louisiana, 70803, United States.

[c] School of Pharmacy and Biomolecular Sciences, University of Brighton, Brighton BN2 4GJ United Kingdom.

Electronic Supplementary Information (ESI) available: Full characterization, experimental details, molecular modelling calculation and X-ray crystallographic data See DOI: 10.1039/b000000x/

1 P. A. Gale, *Coord. Chem. Rev.* 2003**, *240***, 191.
2 P. A. Gale, S. E. García-Garrido, J. Garric, *Chem. Soc. Rev.* 2008**, *37***, 151.
3 P. A. Gale, *Chem. Soc. Rev.* 2010**, *39***, 3746.
4 M. Wenzel, J. R. Hiscock, P. A. Gale, *Chem. Soc. Rev.* 2012**, *41***, 480.
5 P. A. Gale, N. Busschaert, C. J. E. Haynes, L. E. Karagiannidis, I. L. Kirby, *Chem. Soc. Rev.* 2014**, *43***, 205.
6 C. Caltagirone, P. A. Gale, *Chem. Soc. Rev.* 2009**, *38***, 520.
7 Y. M. Hijji, B. Barare, Y. Zhang, *Sens. Actuators, B* 2012**, *169***, 106.
8 A. K. Mahapatra, K. Maiti, P. Sahoo, P. K. Nandi, *J. Lumin.* 2013**, *143***, 349.
9 O. Karagollua, G. Gorur, F. Gode, B. Sennik, F. Yilmazc, *Sens. Actuators, B* 2014**, *193***, 788.
10 D. A. Dzomback, S. B. Roy, T. L. Anderson, M. C. Kavanaugh, R. A. Deeb, "Anthropogenic cyanide in the marine environment". In *Cyanide in Water and Soil (Chemistry, Risk and Management)*, Dzomback, D. A., Ghosh, R. S., Wong-Chong, G. M., Eds. CRC press: Baco Raton, 2006; pp 209.
11 S. D. Ebbs, G. M. Wong-Chong, B. S. Bond, J. T. Bushey, E. F. Neuhauser, "Biological transformation of cyanide in water and soil". In *Cyanide in Water and Soil (Chemistry, Risk and Management)*, Dzomback, D. A., Ghosh, R. S., Wong-Chong, G. M., Eds. CRC press: Baco Raton, 2006; pp 93.
12 G. M. Wong-Chong, D. V. Nakles, D. A. Dzombak, Management of cyanide in industrial process wastewaters. In *Cyanide in Water and Soil (Chemistry, Risk and Management)*, Dzomback, D. A., Ghosh, R. S., Wong-Chong, G. M., Eds. CRC press: Baco Raton, 2006; pp 387.
13 D. A. Dzomback, R. S. Ghosh, T. C. Young, "Physical-chemical properties and reactivity of cyanide in water and soil". In *Cyanide in Water and Soil (Chemistry, Risk and Management)*, Dzomback, D. A., Ghosh, R. S., Wong-Chong, G. M., Eds. CRC press: Baco Raton, 2006; pp 57.
14 K.-S. Lee, H. J. Kim, G.-H. Kim, I. Shin, J.-I. Hong, *Org. Lett.* 2008**, *10***, 49.
15 H. J. Kim, K. C. Ko, J. H. Lee, J. Y. Lee, J. S. Kim, *Chem. Commun.* 2011**, *47***, 2886.
16 W.-C. Lin,S. C. Fang, J.-W. Hu, H.-Y. Tsai, K.-Y. Chen, *Anal. Chem.* 2014, ASAP article.
17 G.-J. Kim, H.-J. Kim, *Tetrahedron Lett.* 2010**, *51***, 2914.
18 S. H. Mashraqui, R. Betkar, M. Chandiramani, C. Estarellas, A. Frontera, *New J. Chem.* 2011**, *35***, 57.
19 R. Tirfoin, S. Aldridge, *Dalton Trans.* 2013**, *42***, 12836.
20 Z. Xu, X. Chen, H. N. Kim, J. Yoon, *Chem. Soc. Rev.* 2010**, *39***.
21 S. Nad, M. Kumbhakar, H. Pal, *J. Phys. Chem. A* 2003**, *107***, 4808.
22 M. Cigáň, J. Donovalová, V. Szöcs, J. Gašpar, K. Jakusová, A. Gáplovský, *J. Phys. Chem. A* 2013**, *117***, 4870.
23 K. J. Wallace, R. I. Fagbemi, F. J. Folmer-Anderson, J. Morey, V. M. Lynch, E. V. Anslyn, *Chem. Commun.* 2006, 3886.
24 P. W. Elsinghorst, W. Hartig, S. Goldhammer, J. Grosche, M. Gutschow, *Org. Biomol. Chem.* 2009**, *7***, 3940.
25 G. Gilli, F. Bellucci, V. Ferretti, B. Bertolasi, *J. Am. Chem. Soc.* 1989**, *111***, 1023.
26 K. J. Wallace, M. Gray, Z. Zhong, V. M. Lynch, E. V. Anslyn, *Dalton Trans.* 2005, 2436.
27 X. Peng, Y. Wu, J. Fan, M. Tian, K. Han, *J. Org. Chem.* 2005**, *70***, 10524.
28 S. Goswami, A. K. Das, K. Aich, A. Manna, *Tetrahedron Lett.* 2013**, *54***, 4215.
29 Y. Wu, X. Peng, J. Fan, S. Gao, M. Tian, J. Zhao, S. Sun, *J. Org. Chem.* 2007**, *72***, 62.
30 U. N. Yadav, P. Pant, D. Sharma, S. K. Sahoob, G. S. Shankarlinga, *Sens. Actuators, B* 2014**, *197***, 73.

31 M. Wang, J. Xu, X. Liu, W. Wang, *New J. Chem.* 2013**,** ***37***, 3869.
32 C. Chakraborty, M. K. Bera, P. Samanta,S. Malik, *New J. Chem.* 2013**,** ***37***, 3222.
33 WHO *"Guidelines for drinking-water quality"*; World Health Organisation: Geneva, Switzaland, 2011; pp 342.
34 P. Rao, P. Singh, S. K. Yadav, N. L. Gujar,R. Bhattacharya, *Food Chem. Toxicol.* 2013**,** ***59***, 595.
35 V. F. Traven, I. V. Ivanov, V. S. Lebedev, T. A. Chibisova, B. G. Milevskii, N. P. Solov´eva,V. I. Polshakov, G. G. Alexandrov,O. N. Kazheva,O. A. Dyachenkod, *Russ. Chem. Bull. Int. Ed.* 2010**,** ***59***, 1605.
36 M. L. Marziaz, K. Frazier, P. B. Guidry, R. A. Ruiz,I. Petrikovics, D. C. Haines, *J. Appl. Toxicol.* 2011**,** ***33***, 50.